Science of the Total Environment 494–495 (2014) 261–271

Contents lists available at ScienceDirect

Science of the Total Environment

journal homepage: www.elsevier.com/locate/scitotenv

Dispersion and fate of ^{90}Sr in the Northwestern Pacific and adjacent seas: Global fallout and the Fukushima Dai-ichi accident

V. Maderich [a,*], K.T. Jung [b], R. Bezhenar [c], G. de With [d], F. Qiao [e], N. Casacuberta [f], P. Masque [g], Y.H. Kim [b]

[a] Institute of Mathematical Machine and System Problems, Glushkov av., 42, Kiev 03187, Ukraine
[b] Korea Institute of Ocean Science and Technology, 787, Haean-ro, Ansan 426-744, Republic of Korea
[c] Ukrainian Center of Water and Environmental Projects, Glushkov av., 42, Kiev 03187, Ukraine
[d] NRG, Utrechtseweg 310, 6800 ES Arnhem, The Netherlands
[e] First Institute of Oceanography, 6 Xianxialing Road, Qingdao 266061, China
[f] Laboratory of Ion Beam Physics, ETH-Zurich, Schafmattstrasse 20, 8093 Zurich, Switzerland
[g] Institut de Ciència i Tecnologia Ambientals & Departament de Física, Universitat Autònoma de Barcelona, 08193 Bellaterra, Spain

HIGHLIGHTS

- A box model with a dynamical food-chain model for the NW Pacific was applied.
- The transport and fate of ^{90}Sr in sea were simulated for the period 1945–2040.
- Marine exposure pathways for ^{90}Sr were assessed for the Fukushima Dai-ichi accident.
- Simulations confirm the presence of leak of ^{90}Sr with a ^{90}Sr/^{137}Cs ratio of about 1.
- ^{90}Sr human dose was 3 orders of magnitude less than that from ^{137}Cs.

ARTICLE INFO

Article history:
Received 28 February 2014
Received in revised form 28 June 2014
Accepted 28 June 2014
Available online 21 July 2014

Editor: Mae Sexauer Gustin

Keywords:
Compartment modeling
Radionuclide transfer in marine biota
Human ingestion doses
Northwestern Pacific
Fukushima Dai-ichi accident
^{90}Sr

ABSTRACT

The 3D compartment model POSEIDON-R was applied to the Northwestern Pacific and adjacent seas to simulate the transport and fate of ^{90}Sr in the period 1945–2010 and to perform a radiological assessment on the releases of ^{90}Sr due to the Fukushima Dai-ichi nuclear accident for the period 2011–2040. The contamination due to runoff of ^{90}Sr from terrestrial surfaces was taken into account using a generic predictive model. A dynamical food-chain model describes the transfer of ^{90}Sr to phytoplankton, zooplankton, molluscs, crustaceans, piscivorous and non-piscivorous fishes. Results of the simulations were compared with observation data on ^{90}Sr for the period 1955–2010 and the budget of ^{90}Sr activity was estimated. It was found that in the East China Sea and Yellow Sea the riverine influx was 1.5% of the ocean influx and it was important only locally. Calculated concentrations of ^{90}Sr in water, bottom sediment and marine organisms before and after the Fukushima Dai-ichi accident are in good agreement with available experimental measurements. The concentration of ^{90}Sr in seawater would return to the background levels within one year after leakages were stopped. The model predicts that the concentration of ^{90}Sr in fish after the Fukushima Dai-ichi accident shall return to the background concentrations only 2 years later due to the delay of the transfer throughout the food web and specific accumulation of ^{90}Sr. The contribution of ^{90}Sr to the maximal dose rate due to the FDNPP accident was three orders of magnitude less than that due to ^{137}Cs, and thus well below the maximum effective dose limits for the public.

1. Introduction

The radioecologically most important long-lived anthropogenic radionuclides in the marine environment are ^{137}Cs (half-life $T_{1/2}$ = 30.2 y) and ^{90}Sr ($T_{1/2}$ = 28.8 y). Both radionuclides are primary fission products; they are highly soluble in seawater and have relatively high bioavailability given the similarities between strontium and calcium (thus accumulation in bones) and caesium and potassium (accumulation in tissues). The vast majority of the inputs of these radionuclides in the oceans is due to global fallout derived from the atmospheric nuclear weapon testing performed in the 1950s and 1960s, quantified in 600 and 380 PBq for ^{137}Cs and ^{90}Sr, respectively (IAEA, 2005), with total inventories estimated in 2010 of 170 and 105 PBq (Povinec et al., 2013). Other sources have been the routine discharges from the reprocessing

* Corresponding author. Tel.: +380 445266084; fax: +380 445263615.
E-mail addresses: vladmad@gmail.com (V. Maderich), ktjung@kiost.ac (K.T. Jung), romanbezhenar@gmail.com (R. Bezhenar), g.dewith@nrg.eu (G. de With), qiaofl@fio.org.cn (F. Qiao), ncasacuberta@phys.ethz.ch (N. Casacuberta), pere.masque@uab.cat (P. Masque), yhkimstar@gmail.com (Y.H. Kim).

http://dx.doi.org/10.1016/j.scitotenv.2014.06.136
0048-9697/

plants and releases resulting from nuclear accidents such as Chernobyl and Fukushima Dai-ichi. The $^{137}Cs/^{90}Sr$ activity ratio caused by global fallout is around 1.5 (UNSCEAR, 2000), but it is different for each of the other sources.

About 50% of the total input of ^{137}Cs and ^{90}Sr into the oceans occurred in the Pacific ocean (IAEA, 2005), due to both its large area and the nuclear weapon testing activities during the mid-XX century in the western equatorial North Pacific (Marshall Islands), where substantial amounts of radionuclides were deposited in the ocean as "close-in fallout" (Bowen et al., 1980). The transport and fate of ^{137}Cs deposited in the Northwestern Pacific and adjacent seas (the East China and Yellow Seas and the East/Japan Sea) due to the nuclear weapon testing were modeled in a number of studies (e.g. Tsumune et al., 2003; Nakano and Povinec, 2003; Nakano, 2006; Nakano et al., 2010; Kawamura et al., 2010; Maderich et al., 2014). However, scarcer modeling studies were devoted to the specific behavior of the ^{90}Sr (Kawamura et al., 2010).

Around 80% of the radioactivity released due to the Fukushima Dai-ichi NPP (FDNPP) accident in March–April 2011 was either directly discharged into the ocean or deposited onto the ocean surface from the atmosphere. The widely accepted estimates for the amount of direct releases of ^{137}Cs from the FDNPP and atmospheric deposition into the ocean lie in the range of 4–6 PBq and 5–15 PBq, respectively (see e.g. Miyazawa et al., 2013). However, in several studies the direct release of ^{137}Cs lies in the range 10–34 PBq (e.g. Rypina et al., 2013; Bailly du Bois et al., 2012). The behavior of ^{137}Cs in water and biota after the accident and the long-term prediction and radiological assessment of ^{137}Cs released in the ocean due to the FDNPP accident has been also documented (Qiao et al, 2011; Nakano and Povinec, 2012; Povinec et al., 2013; Fisher et al., 2013; Maderich et al., 2014). However, the releases of ^{90}Sr from the FDNPP have been studied to a much lesser extent. Several studies estimated the direct releases of ^{90}Sr to the ocean ranging from 40 to 600 TBq (Povinec et al., 2012; Casacuberta et al., 2013; Periañez et al., 2013), and there is evidence that atmospheric deposition of ^{90}Sr due to the FDNPP accident was not the main source of contamination to the ocean (Steinhauser et al., 2013; Casacuberta et al., 2013), since ^{90}Sr is much less volatile than ^{137}Cs. Observed concentrations in seawater were reported by TEPCO (2013), MEXT (2013), Povinec et al. (2012), Casacuberta et al. (2013) and Oikawa et al. (2013), but short-term dynamics of ^{90}Sr was only modeled by Periañez et al. (2013).

The aim of this study is to evaluate the fate and behavior of ^{90}Sr in the Northwestern Pacific and adjacent seas both prior (1945–2010) and after the FDNPP accident (2011–2040). The compartment model POSEIDON-R (Lepicard et al., 2004), recently modified by Maderich et al. (2014), is used for the radiological assessment due to its flexibility for building the compartments in three dimensions. Contrary to most compartment models, where the dose from ingestion of marine products is estimated using the bioconcentration factor (BCF) approach for calculation of the radionuclide concentration in sea organisms, the dose in the POSEIDON-R model is calculated using a dynamical model for the transfer of radionuclides in the food web. This aspect is important for accidental releases characterized by short-term changes with strong spatial gradients of the environmental radioactivity concentration.

The paper is organized as follows: A brief description of the model is given in Section 2. Section 3 presents the model customization for the Northwestern Pacific and adjacent seas. The results of the reconstruction of ^{90}Sr contamination for the period 1945–2010 due to the nuclear weapon testing are given in Section 4. Section 5 discusses the results of the radiological assessment of ^{90}Sr releases into the sea due to the FDNPP accident. Finally, the conclusions are presented in Section 6.

2. Model description

The marine environment in POSEIDON-R is modeled as a system of compartments for water column, bottom sediment and biota (Fig. 1). The compartments describing the water column containing suspended matter are subdivided into a number of vertical layers. The model assumes partition of the radionuclides between the dissolved and particulate fractions in the water column, described by a distribution coefficient. The radionuclide concentration for each compartment is governed by a set of differential equations including the temporal variations of concentration, the exchange with adjacent compartments and with the suspended and bottom sediment, radioactive sources and decay. The exchange between the water column boxes is described by fluxes of radionuclides due to advection, sediment settling and turbulent diffusion processes. The activity on suspended sediment is lost due to settling in underlying compartments and, finally, to the bottom. A three-layer model describes the transfer of radionuclides in the bottom sediment. The transfer of radioactivity from the upper sediment layer (10 cm thickness) to the water column is described by diffusion in

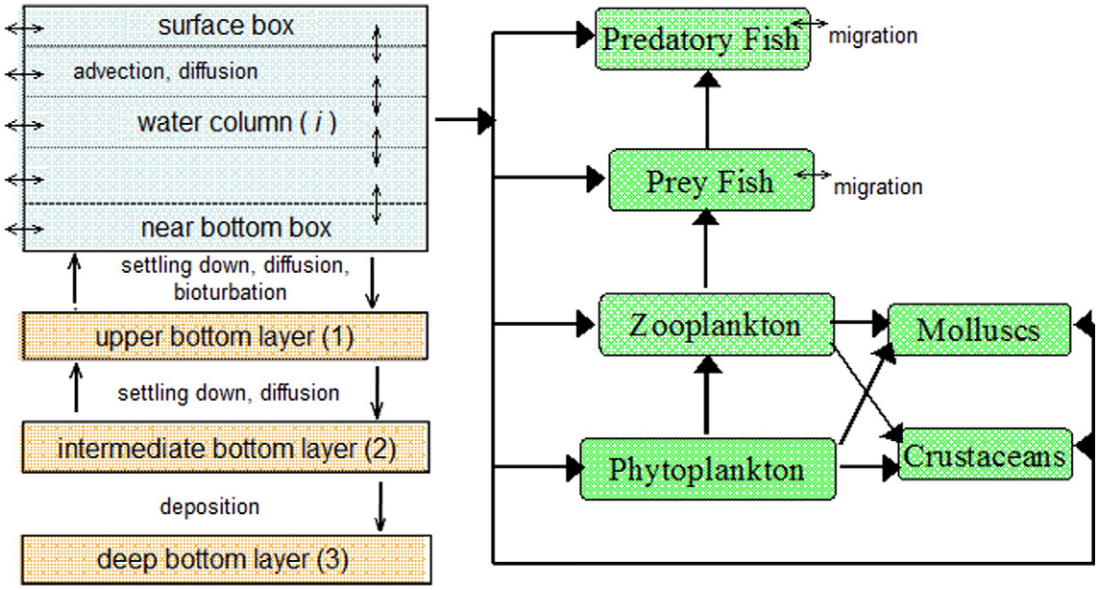

Fig. 1. Scheme of radionuclide transfer in POSEIDON-R model.

the interstitial water and by bioturbation. Radioactivity in the upper sediment layer migrates downwards by diffusion and by burial at a rate taken as the same at which particles settle from the overlying water. The upward transfer of radioactivity from the middle sediment layer to the top sediment layer occurs only by diffusion. Burial causes an effective loss of radioactivity from the middle to the deep sediment layers, from which no upward migration occurs.

The biota model used in POSEIDON-R is the simplified dynamic food web model BURN (Biological Uptake of RadioNuclides) developed by Heling et al. (2002), Heling and Bezhenar (2009) and Maderich et al. (2014), suitable for use in situations which are characterized by rapid temporal changes in environmental concentrations. The detailed description of the BURN model is given in Maderich et al. (2014). Briefly, by grouping the marine organisms in a limited number of classes based on the trophic level and types of species, and by grouping the radionuclides into a limited number of classes associated for fish with the dominating (target) tissue in which a radionuclide accumulates preferably, the number of input parameters is kept limited. Marine organisms are grouped into phytoplankton, zooplankton, fishes (two types: piscivorous and non-piscivorous), crustaceans and molluscs. Due to the rapid uptake and short retention time of radioactivity, the concentration of radionuclides in phytoplankton is calculated using the BCF approach, with a concentration factor of 1 L kg^{-1} for ^{90}Sr (IAEA, 2004). The concentration of a given radionuclide in the zooplankton, fish, crustaceans and molluscs is described by the following differential equation:

$$\frac{dC}{dt} = aK_f C_f + bK_w C_w(t) - K_{0.5} C, \quad (1)$$

where C, C_f and C_w are the radionuclide concentration in the marine organism, food and water, respectively, a is the food extraction coefficient, b is the water extraction coefficient (gills), K_f is the food uptake rate, K_w is the water uptake rate and $K_{0.5}$ is the radionuclide elimination rate from the body. According to Coughtrey and Thorne (1983), radiostrontium uptake through gills decreases with increasing salinity because of higher concentration of competition with Ca^{2+}. This was taken into account in the model by replacing the constant water extraction coefficient b for fish with a relation where b is a function of salinity ($b = 3 \cdot 10^{-5}$ at salinity 34.5), as done by Heling and Bezhenar (2009). The values of b for zooplankton ($1 \cdot 10^{-4}$), molluscs ($1 \cdot 10^{-3}$) and crustaceans ($3 \cdot 10^{-4}$) were chosen from the equilibrium values of BCF for ^{90}Sr recommended by the IAEA (2004).

The POSEIDON-R model can handle four types of radioactive releases: (i) atmospheric deposition directly on the sea surface, (ii) runoff of land deposited radionuclide by river systems, (iii) point sources associated with routine releases from nuclear facilities located either directly at the coast or inland at river systems, and (iv) point sources associated with accidental releases. For coastal discharges occurring in the large ("regional") boxes, "coastal" release boxes are nested into the regional box system. The advection and diffusion of zooplankton are not taken into account, due to its short biological half-life (5 days), except in the coastal box, where diffusion was considered. It was assumed that crustaceans, molluscs, and fish are not transported by ocean flows. When calculating the radionuclide concentration in fish in small coastal boxes, the random fish migration is taken into account (Maderich et al., 2014). For this purpose, the right hand side of Eq. (1) for radionuclide concentration in fish, both in the inner and outer compartments, is extended by the term $(C_{\mathrm{fish}}^{\mathrm{out}} - C_{\mathrm{fish}}^{\mathrm{in}})/T_{migr}$ for the coastal compartment and by the term $-(C_{\mathrm{fish}}^{\mathrm{out}} - C_{\mathrm{fish}}^{\mathrm{in}})/(\delta T_{migr})$, for the outer compartment. Here T_{migr} is the characteristic time of fish migration from a coastal compartment, depending on compartment scale and fish species, and δ is the ratio between the volumes of the outer and the coastal compartments. These relations can be derived from the diffusion equation (Monte, 2002) assuming $T_{migr} \sim l^2 D^{-1}$, where l is the horizontal scale of the inner compartment and D is the diffusion coefficient of random walk. Step-like variations in time of source and boundary conditions are assumed, and the implicit matrix exponential method is used to solve a set of linear ordinary equations of the model.

The individual effective dose rate resulting from the ingestion of five categories of marine products (piscivorous and non-piscivorous fish, crustaceans, molluscs and macro-algae) is calculated for each water compartment using the dose coefficients from ICRP (1995). The macro-algae in the BURN model is not part of the food chain, and thus we used the BCF approach, with a concentration factor of 10 L kg^{-1} (IAEA, 2004) for the calculation of the dose.

3. Model setup for the Northwestern Pacific and adjacent seas

The model was customized for the Northwestern Pacific Ocean, the East China and Yellow Seas and the East/Japan Sea. A total of 176 boxes cover this entire region (Fig. 2). In the deep-sea regions, a three-layer box system was built to describe the vertical and horizontal transports of radioactivity in the upper (0–200 m), intermediate (ocean thermocline, 200–1000 m) and lower (abyssal, >1000 m) layers. The averaged advective and diffusive water fluxes between compartments were calculated for a ten-year period (2000-2009) using the Regional Ocean Modeling System (ROMS), with resolution of 1/9° horizontally and 20 vertical s-levels. The model was nested into the regional North Western Pacific model, which in turn was nested in the global model ECCO. The surface atmospheric forcing was taken from ERA Interim reanalysis. Tidal forcing was applied along the open boundaries. Freshwater discharges from the Chang Jiang and Huang He rivers were included. Details of model setup and forcing are given by Cho et al. (2009). The model validation is given in Cho et al. (2009) and Kim et al. (2014). Averaged over ten-year period, currents in the upper layer of the region were compared in Fig. Supplemental Information 1 (S1) with averaged currents from SODA (Simple Ocean Data Assimilation) reanalysis version 2.2.4 (SODA, 2014). The flow patterns in the ROMS simulation and reanalysis are similar. The characteristic feature of both flow patterns is the Kuroshio Current, transporting water along the eastern coast of Japan to the open ocean. The Kuroshio branch in the East/Japan Sea also transports water to the north and further onto the Pacific Ocean. However, due to the higher resolution of ROMS as compared with SODA, the velocities in boundary currents are greater: the maximum velocity in the Kuroshio calculated by ROMS and SODA is 1.8 m s^{-1} and 0.8 m s^{-1}, respectively. The computed daily velocities have been interpolated to the compartment faces for calculation of the time-averaged advective and diffusive (bi-directional) water fluxes through the surfaces of the connected compartments following the methodology of compartment modeling (e.g. Nielsen, 1995). Following Goshawk et al. (2003), the additional diffusion fluxes were included for boxes in the Yellow Sea to take into account tidal mixing. Concentrations of suspended sediment in the East/Japan Sea and Northwestern Pacific were taken as 1 and 0.1 g m^{-3}, respectively, and sedimentation rates in the East/Japan Sea and Northwestern Pacific were 75 and 10 g m^{-2} y^{-1}, respectively. Concentrations of suspended sediment and sedimentation rates in the Yellow and East China Seas were taken from Choi et al. (2005). More details are given by Maderich et al. (2014).

The contamination due to runoff of ^{90}Sr from terrestrial surfaces can also contribute to the inventory in the ocean. Due to the lack of data for most rivers in the region, we used a generic predictive model (Smith et al., 2004). In this model the concentration of ^{90}Sr in the water of a river is quantified using the exponential "transfer function" model as

$$C_R(t) = \theta \int_{-\infty}^{t} D(\tau)\left(0.984e^{-(\lambda+16)(t-\tau)} + 0.0123e^{-(\lambda+0.09)(t-\tau)} + 0.0037e^{-\lambda(t-\tau)}\right)d\tau, \quad (2)$$

where $C_R(t)$ is the concentration of a radionuclide in the runoff water at time t, $D(t)$ is the global deposition rate of the radionuclide, λ is the radionuclide decay rate, τ is the integration variable, and, θ is the scaling

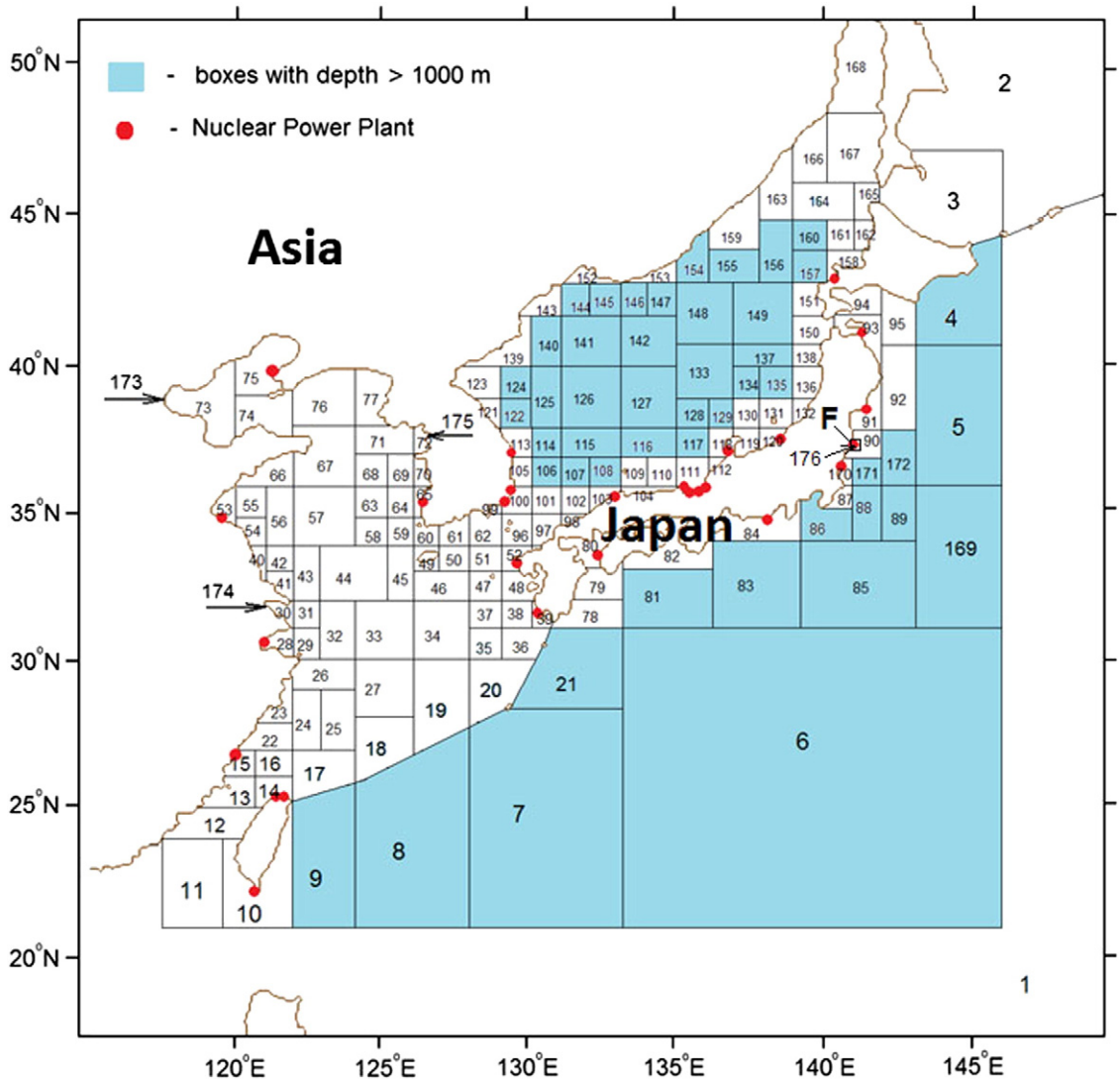

Fig. 2. The compartment system. Shaded boxes represent the deep water boxes (>1000 m). The compartments representing estuaries of large rivers (174 — the Chang Jiang River, 173 — the Huanghe River and 175 — the Han River) are shown by arrows with numbers of compartments. The location of NPPs is indicated by filled circles. Letter "F" represents the Fukushima Dai-ichi NPP. The intermediary regional compartment no. 176 around the FDNPP is also indicated.

factor used to correlate radionuclide runoff with catchment characteristics. This factor was calibrated using measurements of the concentration of ^{90}Sr in river water in Osaka (Ikeuchi, 2003) and in the Han River (Hong et al., 2006). A good agreement was obtained with $\theta = 0.75$, as shown in Fig. S2. This value was used to calculate the concentration of ^{90}Sr in the runoff water from the Chang Jiang (box no. 30), Huanghe (box no. 73) and Han (box no. 72) rivers.

4. Reconstruction of the ^{90}Sr contamination in the East China and Yellow Seas and East/Japan Sea during the period 1945–2010

4.1. Sources of ^{90}Sr

The main source of ^{90}Sr in the Northwestern Pacific during the period 1945–2010 is fallout resulting from atmospheric nuclear weapon tests. The fallout includes global and regional components. The global component in the annual deposition of ^{90}Sr for the period 1945–2000 (Fig. S3A) was compiled from UNSCEAR (2000) for two latitude belts: 40–50°N and 30–40°N, and measurements conducted by the Meteorological Research Institute (MRI) in Tokyo and Tsukuba for 1957–2000 (Igarashi et al., 1996, 2005). The MRI data for the period 1957–1993 agree well with the global data (UNSCEAR, 2000). According to Igarashi et al. (2005) the observations of annual deposition of ^{90}Sr for the period 1990–2000 suggest the presence of a secondary source that is controlled by resuspension of contaminated soil at the continent and, most likely, further aeolian dust deposition from Asia in the Northwestern Pacific.

The concentration of ^{90}Sr in the upper layer of the ocean at the eastern and southern boundaries of the computational domain (see Fig. 2) was estimated using observations from the MARIS (Marine Information System) database (MARIS, 2013) and Povinec et al. (2005). Values of boundary concentration shown in Fig. S3B represent effects of both the global deposition of ^{90}Sr on the Northeastern Pacific and the regional component of deposition from weapon tests carried out at the Marshall Islands (Bikini and Enewetak atolls). The concentration of ^{90}Sr in the intermediate layer of the ocean was set according to observed profiles in the Northwestern Pacific (MARIS, 2013) as 1/5, 1/3 and 1/2 of surface concentration values for the periods 1965–1974, 1975–1984 and 1985–2004, respectively. These values are consistent with the ^{137}Cs distribution in the region (Maderich et al., 2014). As a conservative prediction of the concentration of ^{90}Sr for the period 2000–2010, five-years-averaged deposition over the period 1996–2000 and the boundary concentrations over the period 2000–2004 were extrapolated and corrected for radioactive decay. At the surface

of the model domain the deposition rate of ^{90}Sr was prescribed according to data in Fig. S3A. At the open lateral boundaries of the model domain the concentration of ^{90}Sr in three layers was specified for inflow conditions and it was equal to the compartment value for outflow. The time step for the period 1945–2010 was taken as one year.

4.2. Results

The calculated concentrations of ^{90}Sr in the water column, in the upper layer of the bottom sediment, and in piscivorous fish were compared with observed data wherever possible for the period 1960–2010 in the Northwestern Pacific and adjacent seas. Plot of concentration of ^{90}Sr in the surface layer of the East China in Fig. 3A is an example of the good agreement of the modeled results with available data from MARIS (2013). It was found that the impact of the riverine influx of ^{90}Sr in the East China and Yellow Seas was relatively minor for the boxes adjacent to the Huanghe River (box no. 73) and the Han River (box no. 72), where the difference in concentration was only 17%. However, the riverine influx from Chang Jiang River implied doubling the concentration of ^{90}Sr in box no. 30 (Fig. 3B). Nevertheless, more data for the verification of the riverine model verification would be required, especially for the Chang Jiang River. The calculated concentration of ^{90}Sr in the bottom sediment of the Yellow Sea in 2000 ranged from 0.08 to 0.95 Bq kg^{-1} (boxes no. 53 and 58), whereas observed concentrations by Hong et al. (2006) ranged from <0.5 to 3.7 Bq kg^{-1}.

The calculated budget of ^{90}Sr for the East China and the Yellow Seas for the period 1945–2005 is given in Table S1, being similar to the budget for ^{137}Cs (Maderich et al., 2014). In general, the amount of ^{90}Sr driven to the area by the Pacific Ocean inflow (30.6 PBq, representing about 90% of the input) was balanced by the outflow (30.7 PBq). Global fallout (2.67 PBq) is accounted for 7.9%. However, in the northern part of the Yellow Sea and in the Bohai Sea the contribution of the atmospheric fallout is comparable to the flux driven by weak mean currents in these shallow areas. The outflow occurs mostly via the Tsushima/Korea Strait (28.5 PBq) and a minor fraction (2.2 PBq) of activity returns to the Pacific south of Kyushu Island. The riverine influx (0.54 PBq) was 1.5% and it was of local importance. Only a very small fraction of ^{90}Sr (0.4%) was deposited on the bottom sediment, and 8.5% had decayed. The calculated inventory of ^{90}Sr for the East China Sea and Yellow Sea is given in Table S2 for 2001. The amounts of ^{90}Sr in the water and in the bottom sediment were 0.085 PBq (0.25% from total input) and 0.026 PBq (0.08% from total input), respectively. The amount of ^{90}Sr in water is almost the same as for ^{137}Cs (0.08 PBq), whereas the inventory of ^{90}Sr in the bottom sediment is an order of magnitude smaller than that of ^{137}Cs (0.23 PBq) (Maderich et al., 2014), due to the difference of one order of magnitude between the sediment distribution coefficients of ^{90}Sr and ^{137}Cs.

The estimated concentrations of ^{90}Sr in waters of the East/Japan Sea are represented in Fig. 3C for a shallow region (Korea/Tsushima Strait, box no. 96) and in Fig. 3D for a deep region in the north (box no. 149). The calculated time series agree well with observations (MARIS, 2013) for the surface layer in both regions, as well as for the bottom layer. The calculated ^{90}Sr concentration in the seafloor of the East/Japan Sea in 2001 lies in the range from 0.01 to 4.6 Bq kg^{-1}, whereas observed values range from 0.07 to 1.6 Bq kg^{-1} (Otosaka et al., 2006).

The calculated budget of ^{90}Sr in the East/Japan Sea for the period 1945–2005 is given in Table S1. The inflow from the Tsushima/Korea Strait (28.5 PBq) contributes 91% to the total inputs, while the global fallout (2.78 PBq) is less than 8%. The outflow of ^{90}Sr via the Tsugaru and the Soya Straits (26.7 PBq) balanced inflow (85% of total influx), whereas deposition in the seafloor accounted for only 0.4%. Around 11% of ^{90}Sr has decayed. The inventory of ^{90}Sr in the water column

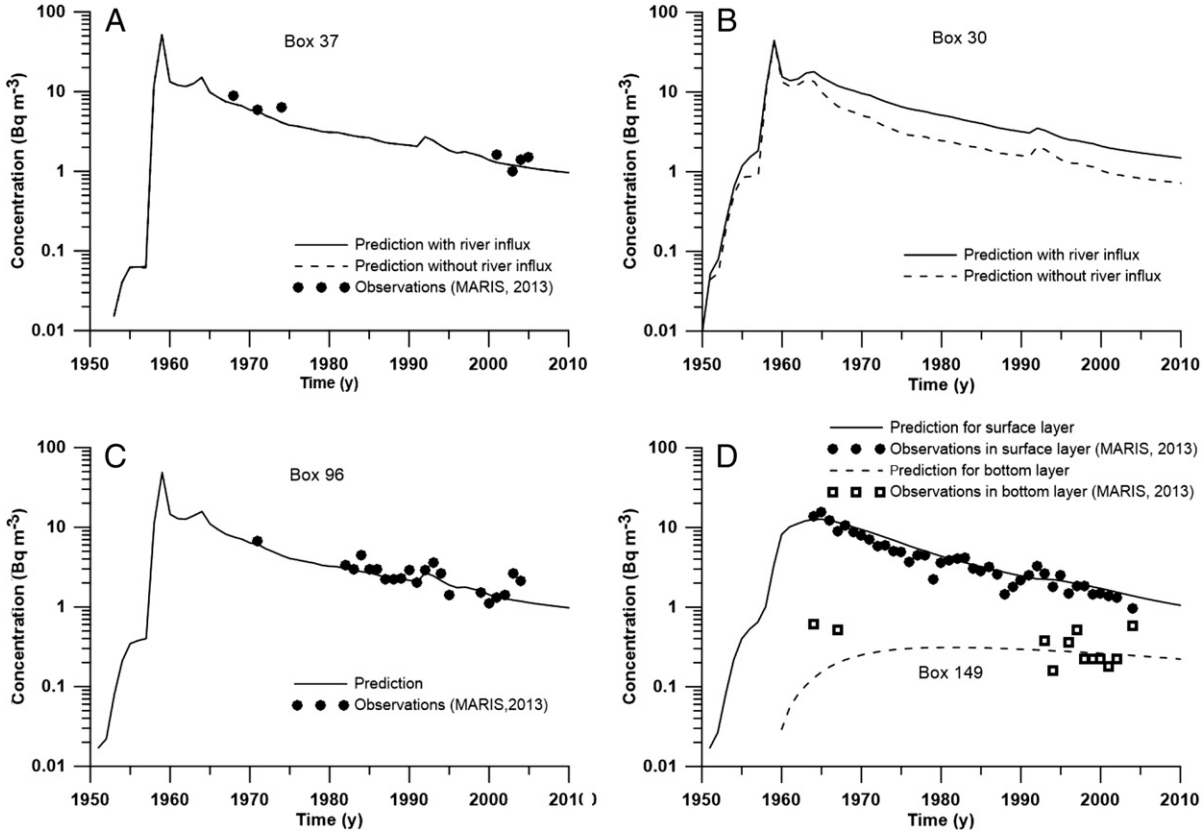

Fig. 3. Calculated concentrations of ^{90}Sr in surface waters for box no. 37 (A) and no. 30 (B) in the East China Sea, and for box no. 96 (C) in the Korea/Tsushima Strait and for box no. 149 (D) in the East/Japan Sea. Predicted concentrations in the East China Sea were estimated with and without considering riverine inputs. Available data from observations as reported in MARIS (2013) are also shown.

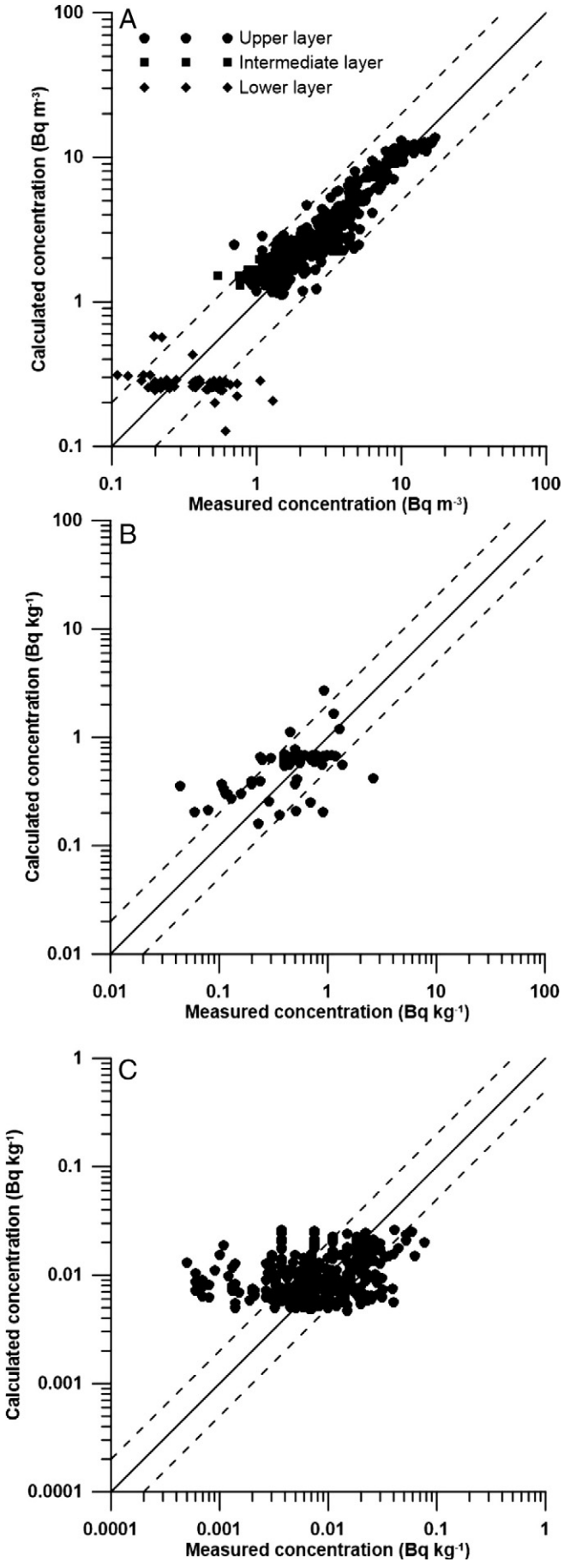

and in the bottom sediment for 2001 is given in Table S2. The calculated inventory in the water column (1.32 PBq) agrees well with the estimates produced by Ito et al. (2007) from measured concentrations (1.16 PBq) as well as with results from modeling (1.34 PBq) conducted by Kawamura et al. (2010). The calculated inventory of ^{90}Sr in the bottom sediment per unit area (64 Bq m^{-2}) lies in the range of the inventories observed by Hong et al. (1999) and Otosaka et al. (2006) (40–70 Bq m^{-2} and 6.8–61 Bq m^{-2}, respectively). However, the calculated total inventory in sediment (0.062 PBq) is higher than the estimate obtained by Ito et al. (2007) (0.016 PBq) for the whole East/Japan Sea.

Calculated values of the concentrations of ^{90}Sr in the water column correlate well (Fig. 4A) with the observed values from the MARIS database (MARIS, 2013). The geometric mean of the predicted-to-observed values is 1.08, with a geometric standard deviation of 1.42 for a total number of observations $n = 490$. These estimates indicate that the model tends to overpredict concentrations in the water column by about 8%, whereas two-third of predicted values ranges within a factor of 1.42 of the observed concentrations. The agreement with observation is better for upper and intermediate layers. The comparison of observed concentrations of ^{90}Sr in the bottom sediment (MARIS, 2013; Hong et al., 2006; Otosaka et al., 2006; MEXT, 2013) and calculations is shown in Fig. 4B. The geometric mean of the predicted-to-observed values is 1.24, with a geometric standard deviation of 1.99 ($n = 62$). The measurements of concentration of ^{90}Sr in piscivorous fish were available only for coastal waters of Japan (MEXT, 2013) for the period 1976–2008. They are compared with calculations in Fig. 4C. The geometric mean of the predicted-to-observed values is 1.20, with a geometric standard deviation is of 2.69 ($n = 285$). The scattering between measured and calculated concentrations of ^{90}Sr in the bottom sediment (Fig. 4B) is greater than for the water column (Fig. 4A). This can be explained through several reasons: (i) use of a single value for the upper layer thickness (10 cm) for all boxes; (ii) use of a single value of the distribution coefficient, 0.2 m3 kg^{-1}, taken from IAEA (2004); (iii) lack of a mechanism of resuspension in the model; and (iv) patchiness of observed concentration distribution. Factors (i)–(iii) can especially affect the results of modeling for the shallow Yellow Sea, where bottom sediment vary from coarse sands to clay. The comparison of experimental data obtained in different studies for the East/Japan Sea (Fig. 3 and Table 4 in Otosaka et al., 2006) shows that inventories in the same areas can differ by an order of magnitude. The inventory estimate for the whole East/Japan Sea by Ito et al. (2007) is based on deep sea data that can result in underestimating the total inventory. These issues need to be resolved in further observations and simulation studies.

5. The impact of the Fukushima Dai-ichi NPP accident

5.1. Sources of ^{90}Sr

To assess the radiological impact of ^{90}Sr on the population for the years to decades following the FDNPP accident, the POSEIDON-R model was customized with the same schematization as for the period 1945–2010 and with the addition of box no. 176 located near the FDNPP and placed within regional box no. 90 (see Fig. 2). The area of this box (30 km along the coast and 15 km across it) is 450 km^2. A smaller coastal box of size 4 × 4 km by the FDNPP was built to describe processes in the vicinity of the power plant. A characteristic time of fish

Fig. 4. Predicted and measured concentrations of ^{90}Sr in the water compartments (A), upper layer of bottom sediment (B) and piscivorous fish (C) for period 1960–2010. The dashed lines correspond to ratios of 2 and 1/2 of predicted-to-measured values. The observed concentrations of ^{90}Sr in the water, sediment and piscivorous fish were taken from MARIS (2013), MARIS (2013), Hong et al. (2006), Otosaka et al. (2006), MEXT (2013), and MEXT (2013), respectively.

migration between boxes (0.67 y) was adopted from Maderich et al. (2014).

The simulation for the period 1945–2010 described in the previous section was continued for the period 2011–2040, including a source term of ^{90}Sr from the FDNPP accident estimated using available data. Determination of this source term is a more complicated task than for the case of ^{137}Cs, because of the absence of measurements of concentrations of ^{90}Sr in direct releases from the FDNPP and the scarcity of data in the sea. The source term estimations for March–May 2011 are based on the assumption that direct releases of ^{90}Sr are proportional to the ^{137}Cs releases. The ratio ^{90}Sr/^{137}Cs was estimated from monitoring data close to the discharge channel (0.01, Povinec et al., 2012), by averaging measurements data for a larger sea area (0.0265, Casacuberta et al., 2013), or from data on water produced during the reactors cooling (i.e. 0.08, Nishimura et al., 2012). The estimates of direct release of ^{137}Cs vary in a range from 4 PBq adopted in many studies (e.g. Nakano and Povinec, 2012) to 10–34 PBq (e.g. Rypina et al., 2013; Bailly du Bois et al., 2012). Using an estimate of 4 PBq, supported by recent reconstruction of ^{137}Cs activity (Tsumune et al., 2014) and the ^{90}Sr/^{137}Cs ratio ranging from 0.01 to 0.08, the direct releases of ^{90}Sr can be estimated to lie in a range from 40 to 320 TBq. The estimations using a 3D model (Periañez et al., 2013) resulted in a value of 80 TBq, which would correspond to the lower end of our estimates. Therefore, we considered three scenarios for the initial releases during the period 1–10 April 2011: 80, 320 and 640 TBq (Fig. S4). The scenario with a larger value of 640 TBq covers possible cases of larger release of ^{90}Sr (see Table 3 from Casacuberta et al., 2013). The direct observations (TEPCO, 2013) after April–May 2011 demonstrated large variations of the concentration of ^{90}Sr in seawater in the vicinity of the discharge channels, which can be related with leaks of radioactivity from the FDNPP. Indeed, the measurements (Povinec et al., 2012; Casacuberta et al., 2013; Oikawa et al., 2013) showed large spatial and temporal variability of the ^{90}Sr/^{137}Cs ratio in seawater. This ratio varied in June–December 2011 in the range of 0.02–0.4 (Oikawa et al., 2013), in August–December 2011 in the range of 0.1–2 (Povinec et al., 2012), and in January–April 2013 in the range of 0.4–2.3 (TEPCO, 2013). The variations of the ^{90}Sr/^{137}Cs activity ratio suggest that ^{90}Sr observed near the FDNPP was originated from leaks of cooling and treated water after removal of radiocaesium by absorbers. Kanda (2013) suggested a continuous leak of 3.6 TBq y^{-1} of ^{137}Cs from the FDNPP in 2012 using the measurements of the concentration of ^{137}Cs in seawater at the harbor of the NPP. The data published by TEPCO (TEPCO, 2013) and the simulation of this leak (Maderich et al., 2014) agreed well, and showed that the leak results in almost constant concentration of ^{137}Cs in the compartment 176 in 2013. Due to the lack of information on the leaks for ^{90}Sr, we used a very conservative scenario, assuming that ^{90}Sr was released at the same rate of 3.6 TBq y^{-1} as ^{137}Cs, i.e. with a ^{90}Sr/^{137}Cs ratio = 1, during the period 2012–2014. Recent estimate of release rates of ^{137}Cs of 10.1 TBq y^{-1} (Tsumune et al., 2014) is not in contradiction with our scenario (see Fig. S4), considering a ^{90}Sr/^{137}Cs ratio of 0.3–0.4 (Masqué et al., 2014). In a similar manner as it was done in the previous section, the boundary concentrations of ^{90}Sr over the period 2000–2004 were extrapolated and corrected for radioactive decay to predict the ^{90}Sr concentration in seawater for the period 2005–2040. The results of long-term simulations of dispersion of ^{137}Cs (Behrens et al., 2012; Nakano and Povinec, 2012) showed significant dilution of the concentration of the radionuclide in the North Pacific after the FDNPP accident. Behrens et al. (2012) estimated that for the release of 10 PBq the concentration of ^{137}Cs in the North Western Pacific would increase in less than 0.3 Bq m^{-3} for the following 3–10 years due to inflow by the North Equatorial Current and Kuroshio (see also Fig. S1). The ^{90}Sr releases from the FDNPP range from 80 to 640 TBq in our scenarios. Therefore, extrapolation of pre-Fukushima time series at open boundary (Fig. S3B), does not lead to a measurable error in our estimates, since the weapon testing origin. Notice that only advection by time-averaged currents is included in the open boundary conditions because the horizontal diffusion describing time-varying and eddy transport plays a minor role in relatively large compartments adjacent to the open boundary.

The time step is governed by step-like variations of the release. Therefore, the time steps for the period 2011–2040 were taken as one day for 1–10 April 2011, one month for 10 April 2011 to end of 2012, three months for 2013–2016, and one year for 2017–2040, without loss of accuracy.

5.2. Results of the simulation for coastal box

The predicted concentrations of ^{90}Sr in the water column and bottom sediment for the coastal box are shown in Fig. 5, together with available measurements. Time series data of the concentrations of ^{90}Sr in the surface water layer before the Fukushima accident were obtained from the Environmental Radiation Database of the Japanese Ministry of Education, Culture, Sports, Science and Technology (MEXT, 2013). Time series data of the concentrations of ^{90}Sr in the water after the Fukushima accident were published by the Tokyo Electric Power Company (TEPCO, 2013), at locations near the discharging channels (T-1 and T-2) and at a distance of about 3 km offshore (T-D5). The model predicts that the concentration of ^{90}Sr in seawater reached a peak due to the releases after the accident and then decreased to reach an equilibrium level of 630 Bq m^{-3} for the period 2012–2015 for all release scenarios (80, 320, 640 TBq). The measurements in Fig. 5A demonstrate high temporal and spatial variability of the concentrations of ^{90}Sr, and confirm the occurrence of releases after April 2011. The average concentration for the period 2012–2013 estimated from measurements at sites T-1, T-2 and T-D5 located in the coastal box area 4 × 4 km is 624 ± 615 Bq m^{-3}. This value corresponds to the model estimated level at a constant leak of ^{90}Sr with a rate of 3.6 TBq y^{-1}. The secondary maximum in December 2011 was pointed out by Povinec et al. (2012) and Casacuberta et al. (2013) as a result of the accidental discharge of treated water. However, our simulation showed that the amount of ^{90}Sr activity released (15 GBq according TEPCO, 2013) was too small to further affect the concentration of ^{90}Sr in the coastal compartment. The simulations showed that when leakages of ^{90}Sr were not to occur

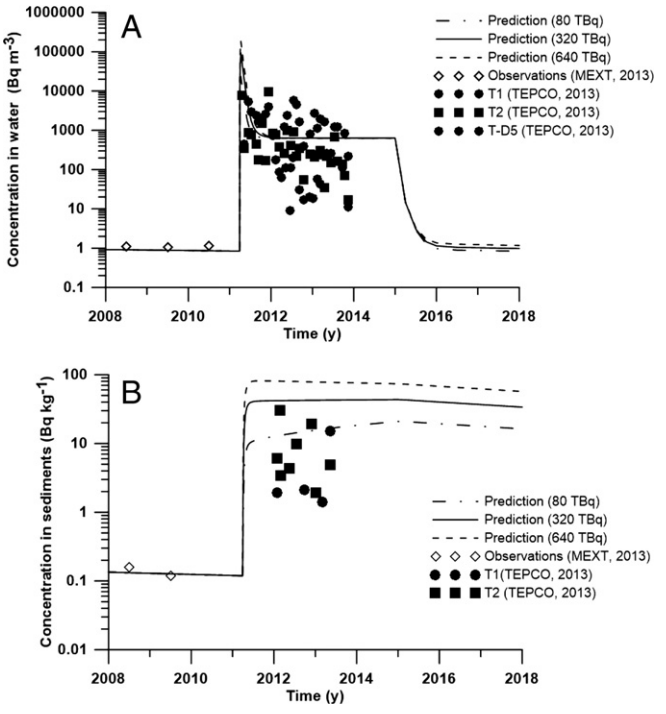

Fig. 5. Comparison between the calculated and observed concentrations of ^{90}Sr in seawater (A) and bottom sediment (B) in the coastal compartment by the FDNPP. Different release scenarios (80, 320 and 640 TBq per year for the period 2012–2014) are considered.

from 2015 onwards, the concentrations of ^{90}Sr in seawater would return to background levels within one year.

The calculated ^{90}Sr concentrations in the bottom sediment of the coastal box before the accident match the measurements carried out by MEXT (Fig. 5B). After the accident, modeled concentrations of ^{90}Sr increased rapidly to values in the range of 10–80 Bq kg^{-1}, depending on which release scenario was considered, and kept increasing slowly during the period 2012–2015. Afterwards they would gradually decrease due to sediment–water exchange and radioactive decay. The observed concentrations in bottom sediment after the accident are highly variable (TEPCO, 2013), ranging from 1.9 to 30 Bq kg^{-1}, with an average value of 10.6 ± 10.3 Bq kg^{-1} for 2012–2013. The observed variability can be a result of patchiness of bottom contamination as mentioned in Section 4.2. The use of different methods of sampling of bottom sediment in shallow areas may lead to integrated different thickness of sampled sediment. The observed average concentration is close to values obtained for the release scenario of 80 TBq, while it is 8 times lower than values obtained for the release scenario of 640 TBq.

The predicted concentrations of ^{90}Sr in non-piscivorous and piscivorous fish in the coastal box near the FDNPP are shown in Fig. 6. The results for piscivorous fish was compared with measurements in fat greenling before the accident (MEXT, 2013) and with data produced by TEPCO (2013) after the accident. The limited sets of TEPCO data represent different kind of piscivorous fishes (shark, skates, rockfish and seabass). The dynamical model predicts a delay in the peak of concentrations of ^{90}Sr in fish that is related to the time needed for the transfer of ^{90}Sr throughout the food web and the long biological life-time in target tissues (bones) for ^{90}Sr (see Maderich et al., 2014). The model predicts that the concentration of ^{90}Sr for both non-piscivorous and piscivorous fish shall return to the background concentrations in 2018, due to the elimination processes governed by the biological life-time and the fish migration into the regional compartment. The results of the simulation show reasonable agreement with observed data before the accident (Fig. 6B). However, even for the greatest release scenario, the model predicts lower values of ^{90}Sr in fish than those determined from the few available measurements. Notice that the model calculates box averaged values of ^{90}Sr concentration in organisms, whereas data shown in Fig. 6B correspond to individual samples. It is likely that most fish moves across the small coastal box and frequents highly contaminated areas near the discharging channels. This phenomenon makes necessary to carry out further studies obtaining and using more data and modeling efforts.

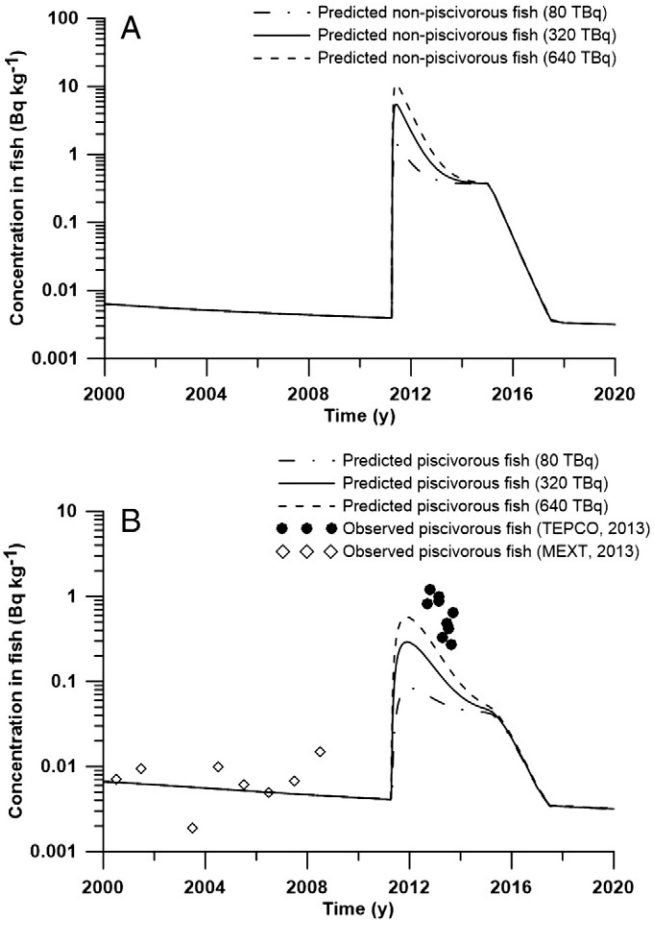

Fig. 6. Predicted concentrations of ^{90}Sr in non-piscivorous fish (A) and piscivorous fish (B) in the coastal box near the FDNPP. Comparison to available data before (MEXT, 2013) and after the accident (TEPCO, 2013) is shown for piscivorous fish.

5.3. Results of the simulation for the intermediary scale box

The predicted concentrations of ^{90}Sr in water and in bottom sediment in the intermediary scale box 176 are shown in Fig. 7. Observation data in a circular-shape area with a radius of 15 km (TEPCO, 2013) showed high concentrations in water after the initial releases. The model predicts the compartment averaged values of concentration, and therefore cannot describe instantaneous values of local concentration in the measurements, even for greatest release scenario (640 TBq). The measurements showed strong variability of ^{90}Sr concentration in water after May 2011, and confirmed the impact of leaks that occurred in 2012–2013 (Fig. 7A). The average concentration for the period 2012–2013 estimated from measurements in sites T-5, T-7, T-8 and T-D9 located in the 15-km area is of 27 ± 20 Bq m^{-3}. The model predicts a constant concentration of ^{90}Sr in water of 26 Bq m^{-3} for

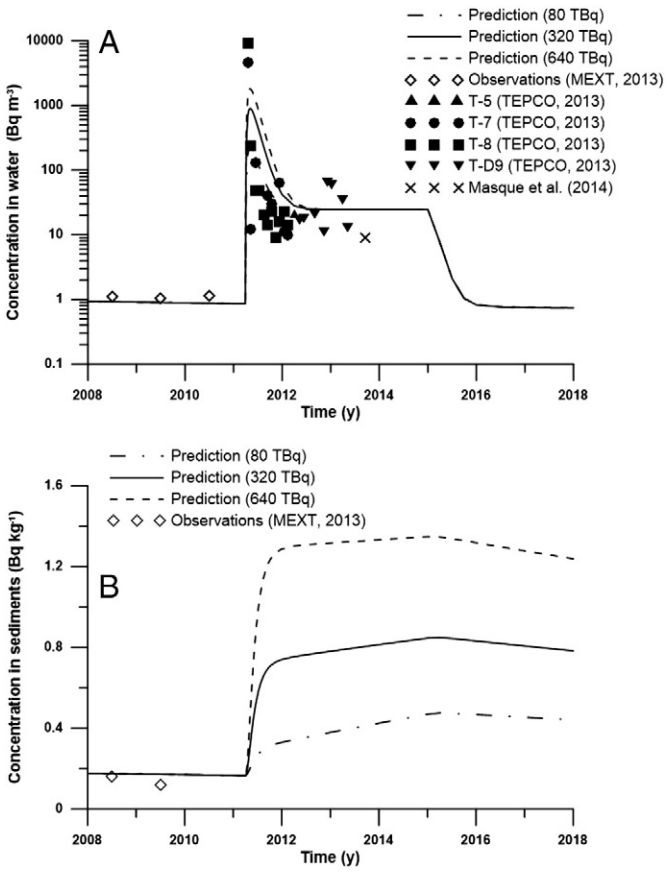

Fig. 7. Comparison between calculated and measured concentrations of ^{90}Sr in surface waters (A) and bottom sediment (B) in box no. 176.

this period for all range of release scenarios, returning to background levels by 2016. It is worth noticing that the concentration of ^{90}Sr during the period 2013–2014 is close to the concentration of ^{137}Cs (20.7 Bq m^{-3}) calculated by Maderich et al. (2014) for the same box.

The predicted concentrations of ^{90}Sr in the upper sediment layer would range from 0.4 to 1.3 Bq kg^{-1} for the different release scenarios (Fig. 7B) for the period 2011–2015, with posterior gradual decline due to exchange and decay processes. The concentration of ^{90}Sr was about three orders of magnitude less that of ^{137}Cs in the upper sediment layer (Maderich et al., 2014), because most of the contamination of the bottom took place by the beginning of April 2011, when concentration of ^{137}Cs in the water was about two orders of magnitude higher than the concentration of ^{90}Sr and due to the differences between ^{137}Cs and ^{90}Sr in kinetics of adsorption to particles.

5.4. Results of the simulation for the regional box

The predicted concentrations of ^{90}Sr in water and in fish in the regional box 90 near the FDNPP for the period 1950–2040 are shown in Fig. 8. The calculated ^{90}Sr concentration in water agrees with measurements published by MEXT (2013) and Watabe et al. (2000) for the period 1964–2010. Regarding the comparison with observations made by MEXT (2013), Casacuberta et al. (2013) and Oikawa et al. (2013) after the accident, again the predicted compartment-averaged concentration for all range of release scenarios was lower than the measured concentrations at several locations inside the box, which we consider is due to the fact that observed values can represent intermittent plumes transported by currents. The predicted concentration of ^{90}Sr in the upper layer of sediment for September–December 2011 (0.18 Bq kg^{-1}) agrees well with observed value (0.17 ± 0.07 Bq kg^{-1}) averaged for this period (Kusakabe et al., 2013) and does not show increase comparatively with the pre-accident value (0.18 Bq kg^{-1}). The predicted concentrations of ^{90}Sr in piscivorous and non-piscivorous fish are given in Fig. 8B for the most conservative scenario of 640 TBq release. These results agree with data (MEXT, 2013) for the period 1984–2010, although there is strong temporal variability of the experimental data resulting in large scatter in Fig. 4C. Notice that averaging the observations and calculations in Fig. 8B for the period 2001–2010 results in almost the same values: 0.0077 and 0.0076 Bq kg^{-1}. The change in the concentration of ^{90}Sr in fish due to the FDNPP accident in the relatively large box 90 is less of 10% of the pre-accident levels, even for the most conservative scenario of a release of 640 TBq.

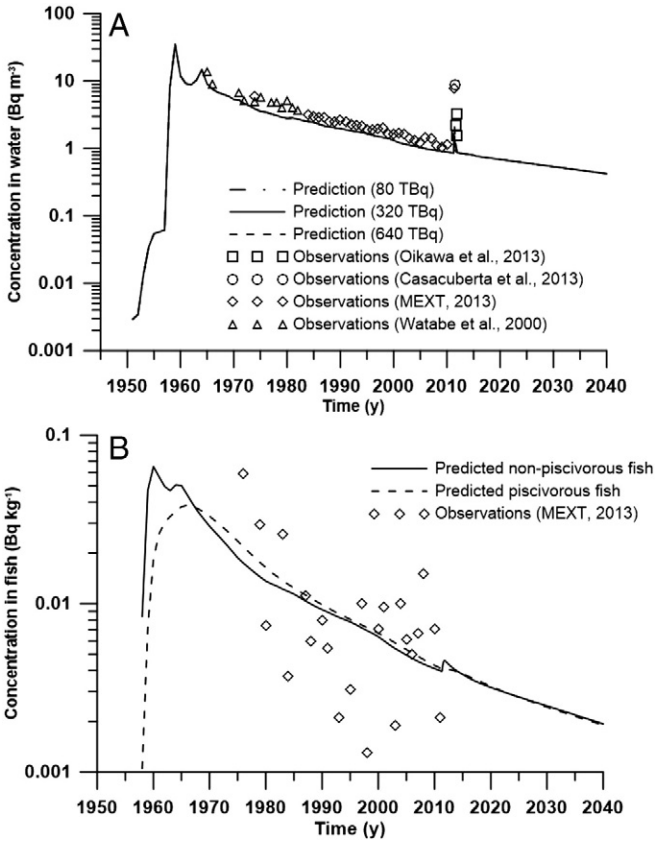

Fig. 8. Predicted ^{90}Sr concentration in seawater (A), and fish for release scenario of 640 TBq (B) in box no. 90 and for the period 1950–2040 . Available data from observations as reported in Watabe et al. (2000), MEXT (2013), Casacuberta et al. (2013) and Oikawa et al. (2013) are also shown.

5.5. Dose estimations

The individual ingestion dose rate due to consumption of contaminated marine products collected from boxes around the FDNPP was estimated on the basis of statistical data on consumption of marine products in Japan as given by Povinec et al. (2013). The annual consumption of marine products per capita is considered to be of 23.4 kg of fish, 2 kg of crustaceans, 1.3 kg of molluscs and 3.7 kg of macro-algae. It was assumed that 60% of consumed fish species are piscivorous and 50% of fish including the bones are consumed for the Far East region (Myoung, 2013).

The calculated individual ingestion dose rates due to consumption of marine products containing ^{90}Sr from boxes 90 and 176 for the period 1950–2040 is shown in Fig. S5 for a conservative release scenario of 640 TBq. Note that marine products from the highly contaminated coastal box (Fig. 6) are not included in this dose estimation. Overall, the relative contribution to the dose rate due to the consumption of the different marine organisms is 47% for fish, 11% for crustaceans, 15% for molluscs, and 27% for macro-algae. However, the relative contributions to the dose due to consumption of marine food for the inner box 176 in 2011 were of only 8% for fish, 26% for crustacean, 15% for molluscs and 50% for macro-algae, due to the different rates of transfer of ^{90}Sr via the food web. The maximal calculated individual dose rates for ^{90}Sr for box 176 due to the FDNPP accident (0.66 μSv y^{-1}) is an order of magnitude greater than the maximal dose rate derived from weapons tests in 1959 (0.045 μSv y^{-1}), which in turn is only 7% of the corresponding dose rate for ^{137}Cs estimated by Maderich et al. (2014). The additional dose rate for box 90 due to FDNPP accident was 20% of the background (weapon tests) value. For box 176, the maximal dose rate due to the FDNPP accident for ^{90}Sr was 3 orders of magnitude less than the corresponding dose rate for ^{137}Cs. Even in the hypothetical worse-case of a reference group that consumed only marine products from the coastal compartment near the FDNPP, the annual dose for 2011 would be of 15 μSv y^{-1}, which is much smaller than the maximum effective dose commitment for public, namely 1 mSv y^{-1} (IAEA, 2011). The dose corresponding to the area including both the coastal and the intermediary scale box can be estimated weighting the input from the coastal box by the ratio of the volumes of the coastal and the intermediary box (0.0143), leading to a maximal annual dose of 0.87 μSv y^{-1}.

6. Conclusions

The 3D compartment model POSEIDON-R (Maderich et al., 2014) was applied to the Northwestern Pacific and adjacent seas to simulate the transport and fate of ^{90}Sr in the period 1945–2010 and to perform a radiological assessment on the releases of ^{90}Sr due to the FDNPP accident for the period 2011–2040. The model predicts the dispersion of radioactivity in the water column and in sediment, and the transfer of radionuclides throughout the marine food web, and the subsequent doses to the population due to the consumption of marine products. The contamination due to runoff of ^{90}Sr from terrestrial surfaces was taken into account using a generic predictive model (Smith et al.,

2004). A dynamical food-chain model describes the transfer of ^{90}Sr to phytoplankton, zooplankton, molluscs, crustaceans, piscivorous and non-piscivorous fishes. The radionuclide uptake model for fish has as a central feature the accumulation of radionuclides in the target tissue (bones for ^{90}Sr).

The model was customized for the Northwestern part of Pacific Ocean, the East China and Yellow Seas, and the East/Japan Sea. Results of the simulations were compared with observation data on ^{90}Sr for the period 1955–2010. The calculations and observations agree well for concentrations in the water column (8% difference), while, some discrepancy between observations and simulation was observed for the sediment and fish was observed (25% and 20%, respectively). The transport by currents dominates the budget of activity. The riverine influx was 1.5% of the ocean influx in the East China and Yellow Seas, and it was only locally important.

To assess the radiological impact of ^{90}Sr as a result of the FDNPP accident, the model was customized with the addition of an intermediate box (no. 176) located within the regional box no. 90, and a small coastal box around the FDNPP. Calculated concentrations of ^{90}Sr in water, bottom sediment and marine organisms in the coastal box around the FDNPP before the accident are in agreement with experimental data. Due to lack of information on the releases of ^{90}Sr from the FDNPP, the scenarios were based on the assumption that the releases of ^{90}Sr and ^{137}Cs are related, but with different ^{90}Sr /^{137}Cs ratios for the initial period (April 2011) and afterwards until 2015. For 2015 we arbitrarily assume that countermeasures will fully prevent leaks of activity from the FDNPP to estimate a period of return to the background state. The comparison of the observation in the coastal box and in box no. 176 with calculations assuming a constant release of 3.6 TBq y^{-1} demonstrate good agreement between time-averaged observations and calculations for the period 2012–2013 and confirm the presence of leaks of ^{90}Sr with a ^{90}Sr/^{137}Cs ratio of about 1. The concentration of ^{90}Sr in seawater would return to the background levels within one year after leakages were stopped. The concentrations of ^{90}Sr in the sediment and in the biota largely depend on the initial release in April 2011, when concentrations in bottom sediment increased rapidly, and only after 2015 they would gradually decrease. The dynamical food web model predicts that due to the delay of the transfer throughout the food web and specific accumulation of ^{90}Sr, the concentration for both non-piscivorous and piscivorous fish shall return to background levels only in 2018. The remaining question is the amount of initially released ^{90}Sr. The comparison between observations and simulation for the sediment in the coastal compartment suggests a lower value of released ^{90}Sr (80 TBq), in good agreement with the estimate obtained by Periañez et al. (2013). However, observed concentrations in fish are greater than those simulated here, even for the most conservative scenario (640 TBq). The relative contribution to the dose rate due to the consumption of the different marine organisms before the accident and in 2011 differs due to different rates of transfer of ^{90}Sr via the food web. Nevertheless, the impact of ^{90}Sr in the maximal dose rate due to the FDNPP accident was three orders of magnitude less than the dose derived from ^{137}Cs and well below the maximum effective dose commitment.

Acknowledgments

This work was supported by KIOST project “Development of the marine environmental impact prediction system following the disastrous environmental event”, CKJORC (China–Korea Joint Ocean Research Center) Project for Nuclear Safety, FP7-Fission-2012 project PREPARE “Innovative integrative tools and platforms to be prepared for radiological emergencies and post-accident response in Europe” and it is in the frame of IAEA MODARIA Programme “Modelling and data for radiological impact assessments”. PM acknowledges funding through the Ministerio de Ciencia e Innovación of Spain (CTM2011-15152-E) and the Generalitat de Catalunya through the ICREA Academia prize. This article benefited from the comments and suggestions of four anonymous reviewers.

Appendix A. Supplementary data

Supplementary data to this article can be found online at http://dx.doi.org/10.1016/j.scitotenv.2014.06.136.

References

Bailly du Bois P, Laguionie P, Boust D, Korsakissok I, Didier D. Estimation of marine source-term following Fukushima Dai-ichi accident. J Environ Radioact 2012;114:2–9.
Behrens E, Schwarzkopf FU, Lübbecke JF, Böning CW. Model simulations on the long-term dispersal of ^{137}Cs released into the Pacific Ocean off Fukushima. Environ Res Lett 2012;7:034004. http://dx.doi.org/10.1088/1748-9326/7/3/034004.
Bowen VT, Noshkin VE, Livingston HD, Volchok HL. Fallout radionuclides in the Pacific Ocean: vertical and horizontal distributions, largely from GEOSEC stations. Earth Planet Sci Lett 1980;49:411–34.
Casacuberta N, Masqué P, Garcia-Orellana J, Garcia-Tenorio R, Buesseler KO. ^{90}Sr and ^{89}Sr in seawater off Japan as a consequence of the Fukushima Dai-ichi nuclear accident. Biogeosciences 2013;10:3649–59. http://dx.doi.org/10.5194/bg-10-3649-2013.
Cho Y-K, Seo G-H, Choi B-J, Kim S, Kim Y-G, Youn Y-H, et al. Connectivity among straits of the Northwestern Pacific marginal seas. J Geophys Res 2009;114:C06018. http://dx.doi.org/10.1029/2008JC005218.
Choi BH, Mun JY, Ko JS, Yuk JH. Simulation of suspended sediment in the Yellow and East China Seas. China Ocean Engineering 2005;19:235–50.
Coughtrey PJ, Thorne MC. Radionuclide distribution and transport in terrestrial and aquatic ecosystems: a critical review of data. vol. 1. Rotterdam: A A Balkema; 1983.
Fisher NS, Beaugelin-Seiller K, Hinton TG, Baumann Z, Madigan DJ, Garnier-LaPlace J. Evaluation of radiation doses and associated risk from the Fukushima nuclear accident to marine biota and human consumers of seafood. Proc Natl Acad Sci U S A 2013. http://dx.doi.org/10.1073/pnas.1221834110.
Goshawk JA, Clarke S, Smith CN, McDonald P. MEAD (Part I) – a mathematical model of the long-term dispersion of radioactivity in shelf sea environments. J Environ Radioactivity 2003;68:115–35.
Heling R, Bezhenar R. Modification of the dynamic radionuclide uptake model BURN by salinity driven transfer parameters for the marine foodweb and its integration in POSEIDON-R. Radioprotection 2009;44:741–6.
Heling R, Koziy L, Bulgakov V. On the dynamical uptake model developed for the uptake of radionuclides in marine organisms for the POSEIDON-R model system. Radioprotection 2002;37(C1):833–8.
Hong GH, Lee SH, Kim SH, Chung CS, Baskaran M. Sedimentary fluxes of ^{90}Sr, ^{137}Cs, ^{239,240}Pu and ^{210}Pb in the East Sea (Sea of Japan). Sci Total Environ 1999;237/238:225–40.
Hong GH, Chung CS, Lee SH, Kim SH, Baskaran M, Lee HM, et al. Artificial radionuclides in the Yellow Sea: inputs and redistribution. Radioact Environ 2006;8:96–133.
IAEA International Atomic Energy Agency. Sediment distribution coefficients and concentration factors for biota in the marine environment. Technical Report Series No 422. Vienna, Austria: IAEA; 2004.
IAEA International Atomic Energy Agency. Worldwide marine radioactivity studies (WOMARS). Radionuclide levels in oceans and sea. Vienna, Austria: IAEA-TECDOC-1429 IAEA; 2005.
IAEA International Atomic Energy Agency. Radiation protection and safety of radiation sources: international basic safety standards. General safety requirements. Interim ed. Vienna, Austria: IAEA; 2011.
ICRP International Commission on Radiological Protection. Age-dependent doses to the members of the public from intake of radionuclides. Part 5: Compilation of ingestion and inhalation coefficients. Paris: Publication 72 ICRP; 1995.
Igarashi Y, Otsuji-Hatori M, Hirose K. Recent deposition of ^{90}Sr and ^{137}Cs observed in Tsukuba. J Environ Radioact 1996;31:157–69.
Igarashi Y, Aoyama M, Hirose K, Povinec P, Yabuki S. What anthropogenic radionuclides (^{90}Sr and ^{137}Cs) in atmospheric deposition, surface soils and aeolian dusts suggest for dust transport over Japan. Water Air Soil Pollut Focus 2005;5:51–69.
Ikeuchi Y. Temporal variations of ^{90}Sr and ^{137}Cs concentrations in Japanese coastal surface seawater and sediments from 1974 to 1998. Deep Sea Res Part II 2003;50:2713–28.
Ito T, Otosaka S, Kawamura H. Estimation of total amounts of anthropogenic radionuclides in the Japan Sea. J Nucl Sci Tech 2007;44(6):912–22.
Kanda J. Continuing ^{137}Cs release to the sea from the Fukushima Dai-ichi Nuclear Power Plant through 2012. Biogeosciences 2013;10:6107–13.
Kawamura H, Ito T, Kobayashi T, Otosaka S, Hirose N, Togawa O. Numerical experiment for Strontium-90 and Cesium-137 in the Japan Sea. J Oceanogr 2010;66:649–62.
Kim C-S, Cho Y-K, Seo G-H, Choi B-J, Jung K-T, Lee B-G. Interannual variation of freshwater transport and its causes in the Korea Strait: a modeling study. J Mar Syst 2014;132:66–74.
Kusakabe M, Oikawa S, Takata H, Misonoo J. Spatiotemporal distributions of Fukushima-derived radionuclides in nearby marine surface sediments. Biogeosciences 2013;10:5019–30. http://dx.doi.org/10.5194/bg-10-5019-2013.
Lepicard S, Heling R, Maderich V. POSEIDON-R/RODOS models for radiological assessment of marine environment after accidental releases: application to coastal areas of the Baltic, Black and North Seas. J Environ Radioact 2004;72:153–61.
Maderich V, Bezhenar R, Heling R, Jung KT, Myoung JG, Cho Y-K, et al. Regional long-term model of radioactivity dispersion and fate in the Northwestern Pacific and adjacent

seas: application to the Fukushima Dai-ichi accident. J Environ Radioact 2014;131:4–18.
MARIS, Marine Information System. Data available at http://maris.iaea.org/, 2013.
Masqué P, Casacuberta N, Pike S, Castrillejo M, Buesseler KO. Evolution of Cs-137, Cs-134 and Sr-90 in the Pacific Ocean derived from the Fukushima Dai-ichi nuclear accident. 2014 Ocean Sciences Meeting. Honolulu (USA), 23–28 February 2014; 2014.
MEXT. Japanese Ministry of Education, Culture, Sports, Science and Technology. Environmental radiation database; 2013 [Data available at http://search.kankyo-hoshano.go.jp/servlet/search.top].
Miyazawa Y, Masumoto Y, Varlamov SM, Miyama T, Takigawa M, Honda M, et al. Inverse estimation of source parameters of oceanic radioactivity dispersion models associated with the Fukushima accident. Biogeosciences 2013;10:2349–63. http://dx.doi.org/10.5194/bg-10-2349-2013.
Monte L. A methodology for modelling the contamination of moving organisms in water bodies with spatial and time dependent pollution levels. Ecol Modell 2002;158:21–33.
Myoung JG. Personal communication; 2013.
Nakano M. Simulation of the advection–diffusion–scavenging processes for ^{137}Cs and ^{239,240}Pu in the Japan Sea. Radioact Environ 2006;8:433–48.
Nakano M, Povinec PP. Oceanic general circulation model for the assessment of the distribution of ^{137}Cs in the world ocean. Deep Sea Res Part II 2003;50:2803–16.
Nakano M, Povinec PP. Long-term simulations of the ^{137}Cs dispersion from the Fukushima accident in the world ocean. J Environ Radioact 2012;111:109–15.
Nakano H, Motoi T, Hirose K, Aoyama M. Analysis of ^{137}Cs concentration in the Pacific using a Lagrangian approach. J Geophys Res 2010;115:C06015. http://dx.doi.org/10.1029/2009JC005640.
Nielsen SP. A box model for North-East Atlantic coastal waters compared with radioactive tracers. J Mar Syst 1995;6:545–60.
Nishihara K, Yamagishi I, Yasuda K, Ishimori K, Tanaka K, Kuno T, et al. Radionuclide release to stagnant water in Fukushima-1 nuclear power plant. At Energy Soc Jpn 2012;11(1):13–9.
Oikawa S, Takata H, Watabe T, Misonoo J, Kusakabe M. Distribution of the Fukushima-derived radionuclides in seawater in the Pacific off the coast of Miyagi, Fukushima, and Ibaraki Prefectures, Japan. Biogeosciences 2013;10:5031–47. http://dx.doi.org/10.5194/bg-10-5031-2013.
Otosaka S, Amano H, Ito T, Kawamura H, Kobayashi T, Suzuki T, et al. Anthropogenic radionuclides in sediment in the Japan Sea: distribution and transport processes of particulate radionuclides. J Environ Radioact 2006;91:128–45.
Periañez R, Suh K-S, Min B-I, Casacuberta N, Masque P. Numerical modelling of the releases of ^{90}Sr from Fukushima to the ocean: an evaluation of the source term. Environ Sci Technol 2013. http://dx.doi.org/10.1021/es4031408.
Povinec PP, Aarkrog A, Buesseler KO, Delfanti R, Hirose K, Hong G-H, et al. ^{90}Sr, ^{137}Cs and ^{239,240}Pu concentration surface water time series in the Pacific and Indian Oceans — WOMARS results. J Environ Radioact 2005;81:63–87.
Povinec PP, Hirose K, Aoyama M. Radiostrontium in the western North Pacific: characteristics, behavior, and the Fukushima impact. Environ Sci Technol 2012;46:10356–63. http://dx.doi.org/10.1021/es301997c.
Povinec P, Hirose K, Aoyama M. Fukushima accident: radioactivity impact on the environment. Elsevier; 2013.
Qiao FL, Wang GS, Zhao W. Predicting the spread of nuclear radiation from damaged Fukushima Nuclear Power Plant. Chin Sci Bull 2011;56(18):1890–6.
Rypina II, Jayne SR, Yoshida S, Macdonald AM, Douglass E, Buesseler K. Short-term dispersal of Fukushima-derived radionuclides off Japan: modeling efforts and model-data intercomparison. Biogeosciences 2013;10:4973–90.
Smith JT, Wright SM, Cross MA, Monte L, Kudelsky AV, Saxén R, et al. Global analysis of the riverine transport of ^{90}Sr and ^{137}Cs. Environ Sci Technol 2004;38:850–7.
SODA Simple Ocean Data Assimilation. A reanalysis of ocean climate; 2014 [Data available at http://www.atmos.umd.edu/~ocean].
Steinhauser G, Schauer V, Shozugawa K. Concentration of Strontium-90 at selected hot spots in Japan. PLoS One 2013;8(3):e57760. http://dx.doi.org/10.1371/journal.pone.0057760.
TEPCO Tokyo Electric Power Company. Current situation of Fukushima Daiichi and Daini nuclear power station; 2013 [Data available at http://www.tepco.co.jp/en/nu/fukushima-np/index-e.html].
Tsumune D, Aoyama M, Hirose K. Behavior of ^{137}Cs concentrations in the North Pacific in an ocean general circulation model. J Geophys Res 2003;108(C8):3262. http://dx.doi.org/10.1029/2002JC001434.
Tsumune D, Aoyama M, Tsubono T, Tateda Y, Misumi K, Hayami H, et al. Reconstruction of ^{137}Cs activity in the ocean following the Fukushima Daiichi Nuclear Power Plant accident. Geophys Res Abstr 2014;16:EGU2014–9566.
UNSCEAR United Nations Scientific Committee on the Effect of Atomic Radiation. Exposures of the public from man-made sources of radiation. Sources and Effects of Ionizing Radiation. New York: United Nations; 2000.
Watabe T, Matsuba M, Yokosuka S. Fate of two important radionuclides in the coastal seas of Japan and resultant dose from intake through fishery products. Proc 10th Int Cong of Int Radiat Prot Assoc; 2000. p. 4–244.